there is better agreement between numerical, experimental, and asymptotic results. In Table 1, calculated values of P and P' are compared with the data of Chapman et al.[1] Again, it is noted that, while the results for P' agree very well, those for P do not. This may be due to experimental inaccuracies in the location of the separation point magnified by scaling factors. A more disconcerting discrepancy is that as the Reynolds number increases, the numerical value of pressure at separation moves away from the asymptotic value. As in the case of incipient separation, the discrepancy between numerical and asymptotic results is due to the fact that the 32×32 grid does not resolve the interaction region sufficiently. To improve resolution, the computations were carried out on a 128×32 grid with other parameters unchanged. Figures 3 and 4 present the pressure and skin-friction distributions in the free-interaction region for Reynolds number equal to 0.04×10^6 and 0.4×10^6. Results for the intermediate values of Reynolds number fall consistently between those shown. The scaled pressure P at separation ($x=0$) now approaches the asymptotic value as the Reynolds number increases. It should be noted that in the asymptotic analysis, p_0 is the surface pressure in the Blasius case and is equal to the freestream pressure. In the numerical computations for finite Reynolds number, the surface pressure p_b is different from p_0 due to the effect of boundary-layer displacement thickness. In Fig. 3, the scaled pressure P is referred to p_b instead of p_0, and hence, P tends to zero ahead of the interaction region, whereas the scaled pressure based on p_0 would not tend to zero.

Conclusions

For the range of physical and numerical parameters considered, numerical methods of the type employed here are accurate enough for practical purposes. Moreover, it can generally be concluded that the asymptotic theory[5] is useful as a test bed for numerical schemes developed for computation of complex flow configurations for design purposes. The mesh resolution suggested by the asymptotic scaling laws are of value in numerical simulation codes which are expected to yield reliable results difficult to obtain in the laboratory. Application of a numerical method to simple problems, which may not necessarily be of practical importance but which possess precise solutions, can help in evaluating the capabilities and limitations of the method.

Acknowledgment

The first author was partially supported under NASA Contracts NAS1-14101 and NAS1-14472 while in residence at ICASE, NASA Langley Research Center, Hampton, Va.

References

[1] Chapman, D. R., Kuehn, D. M., and Larson, H. K., "Investigation of Separated Flows in Supersonic and Subsonic Streams with Emphasis on the Effects of Transition," NACA Rept. 1356, 1958.

[2] Lighthill, M. J., "On Boundary Layers and Upstream Influence. A Comparison between Subsonic and Supersonic Flows," *Proceedings of the Royal Society, London*, Vol. A217, May 1953, pp. 478-507.

[3] Stewartson, K. and Williams, P. G., "Self-Induced Separation," *Proceedings of the Royal Society, London*, Vol. A312, Sept. 1969, pp. 181-206.

[4] Neiland, V. Y., "Towards a Theory of Separation of a Laminar Boundary Layer in Supersonic Stream," *Izvestia Akademii Nauk SSSR, Mekhanika Zhidkostii Gaza*, Vol. 4, No. 4, 1969 (*Fluid Dynamics*, Vol. 4, No. 4, July 1969, pp. 33-35).

[5] Stewartson, K., "Multistructured Boundary Layers on Flat Plates and Related Bodies," *Advances in Applied Mechanics*, Vol. 14, Academic Press, Inc., New York, 1974, pp. 145-239.

[6] MacCormack, R. W., "An Efficient Explicit-Implict-Characteristic Method for Solving the Compressible Navier-Stokes Equations," *SIAM-AMS Proceedings*, Vol. 11, 1978, pp. 130-155.

[7] Sychev, V. V., "Laminar Separation," *Izvestia Akademii Nauk SSSR, Mekhanika Zhidkostii Gaza*, Vol. 7, No. 3, May 1972, pp. 407-417.

[8] Ragab, S. A. and Nayfeh, A. H., A Second-Order Asymptotic Solution for the Laminar Separation of Supersonic Flows Past Compression Ramps," AIAA Paper 78-1132, Seattle, Wash., July 1978.

[9] Hakkinen, R. J., Trilling, G. L., and Abarbanel, S. S., "The Interaction of an Oblique Shock Wave with a Laminar Boundary Layer," NASA Memo 2-18-59W, March 1959.

Mach and Reynolds Number Effects on a Shock-Wave/Boundary-Layer Interaction

G. G. Mateer* and J. R. Viegas†
NASA Ames Research Center, Moffett Field, Calif.

Nomenclature

c_f = skin friction coefficient
M = Mach number
p = pressure
Re = Reynolds number
x = axial coordinate
δ = boundary-layer thickness

Subscripts

s = distance along tunnel wall
∞ = freestream value just ahead of the shock wave

Introduction

THE present investigation was undertaken as part of a continuing experimental/numerical program to evaluate and improve turbulence models for use in Navier-Stokes (N-S) codes. The normal shock-wave/turbulent boundary-layer interaction is a good test for such computations because it contains strong adverse pressure gradients and the possibility of local flow separation.

Experimental studies of these interactions are usually conducted on wind tunnel walls or large flat plates that have thick, easily documented boundary layers. However, the constraining effect of the tunnel walls may prevent the flow from developing as it would in free air.[1] Since constraints must be included in any computational scheme, methods employing the N-S equations are attractive because simultaneous treatment of both the viscous and inviscid flowfields is possible. The evolution of N-S codes is based primarily upon the development of models for the turbulence terms in these equations. Earlier work[2] provided a data base at single Mach and Reynolds numbers which was used[3] to evaluate various types of eddy viscosity models of the turbulence (algebraic, one-, and two-equation, etc.). In the present study of the most promising model[4] is tested over a wider range of Mach and Reynolds numbers.

Presented as Paper 79-1502 at the AIAA 12th Fluid and Plasma Dynamics Conference, Williamsburg, Va., July 23-25, 1979; submitted Aug. 27, 1979; revision received Jan. 21, 1980. This paper is declared a work of the U.S. Government and therefore is in the public domain.

Index categories: Transonic Flow; Boundary Layers and Convective Heat Transfer—Turbulent; Computational Methods.

*Research Scientist.

†Research Scientist. Member AIAA.

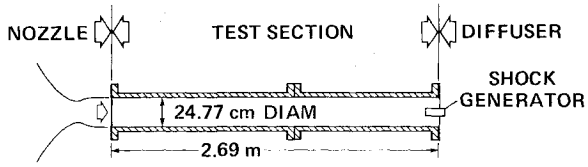

Fig. 1 Geometry.

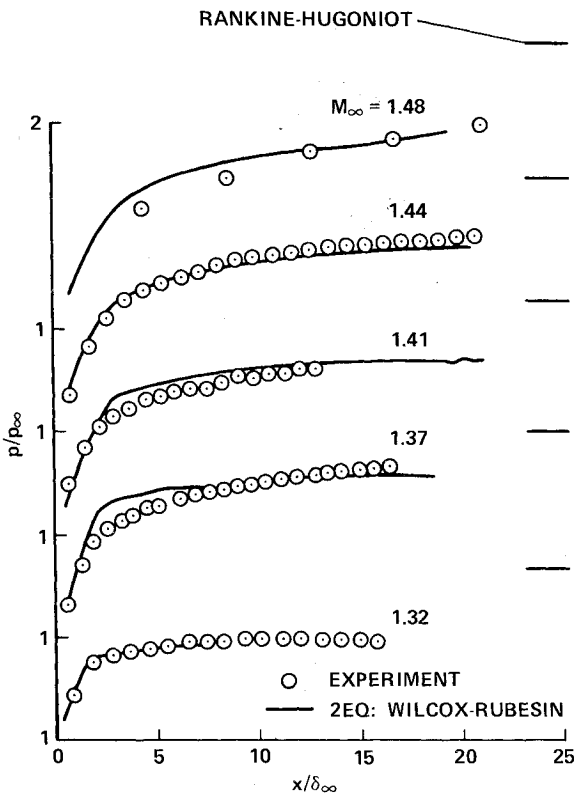

Fig. 2 Effect of Mach number on pressure, $Re_s = 20 \times 10^6$.

Apparatus and Test Conditions

The experiment was conducted in the high Reynolds number channel[5] at Ames Research Center. A nominal Mach 1.5 nozzle was used in conjunction with a 2.69-m-long test section of constant diameter (24.77 cm, see Fig. 1). A normal shock wave was positioned inside the test section by inserting a shock-wave generator into the exit. The distance between the shock wave and the generator was typically 2 m.

The facility was operated in the blowdown mode using air at a nominal temperature of 283 K. Total pressure ranged from 0.34 to 5.44 atm. Two sets of data were obtained, one at constant $M_\infty = 1.42$ ($8.5 \times 10^6 \leq Re_s \leq 2.25 \times 10^6$) and one at $Re_s = 20 \times 10^6$ ($1.32 \leq M_\infty \leq .48$).

The interaction was documented at the wall by measuring the pressure, shear stress, and flow direction. Shear stress was determined by using the buried wire technique.[6] The direction of fluid motion near the wall was measured using an unobtrusive method described in Ref. 6.

The computational procedures are identical to those in Ref. 3. The control volume includes the interaction and extends from the walls to the centerline of the tube. Details of typical computational grids and boundary conditions are described in Refs. 2 and 3.

Results and Discussion

The effect of Mach number on wall static pressure is shown on Fig. 2. The distance x is measured from the initial pressure rise. The pressure increases abruptly through the interaction and reaches a level that is below the Rankine-Hugoniot value.

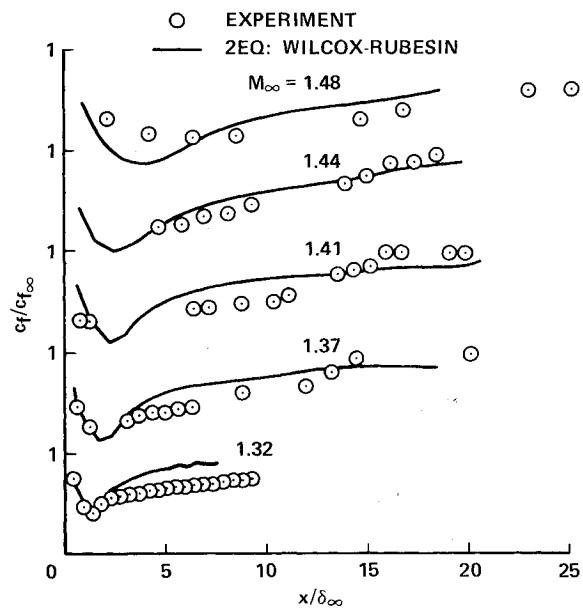

Fig. 3 Effect of Mach number on skin friction, $Re_s = 20 \times 10^6$.

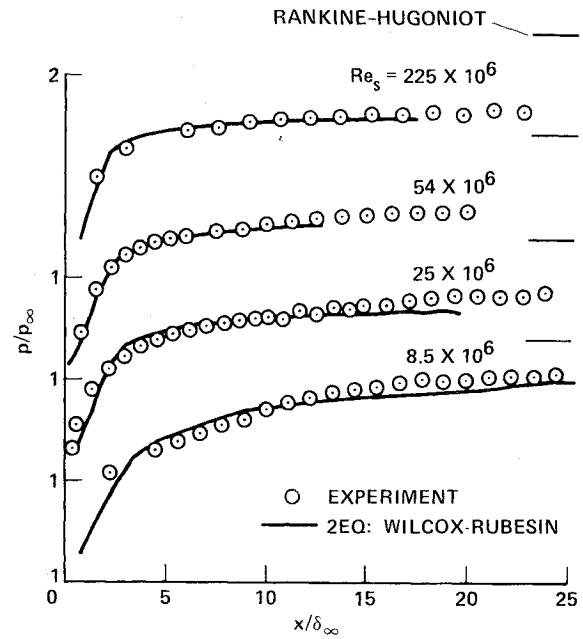

Fig. 4 Effect of Reynolds number on pressure, $M_\infty = 1.42$.

This reduced pressure is the result of the wall boundary layer effectively decreasing the diameter of the test section. As M_∞ increases there is a reduction in the presure gradient at the shock and an augmentation in the downstream pressure ratio. The accompanying effect on skin friction is illustrated in Fig. 3 as a decrease in the minimum value of c_f and a movement of this minimum downstream. These effects are estimated quite well by the computations; however, a very small separation bubble is predicted for $M_\infty = 1.48$. This feature was not observed in either the c_f or flow direction data. However, if such a bubble did exist and was undergoing unsteady motion greater than 1 kHz (the response limit of the sensors), it could not have been detected.

The effect of Reynolds number on the wall static pressure is shown on Fig. 4. Increasing Re_s steepens the pressure gradient at the shock and reduces the downstream pressure ratio. The skin friction data on Fig. 5 reflect the initial increase in Re_s as an abrupt increase in c_f throughout the interaction; however, subsequent increases in Re_s have very little effect on c_f. The

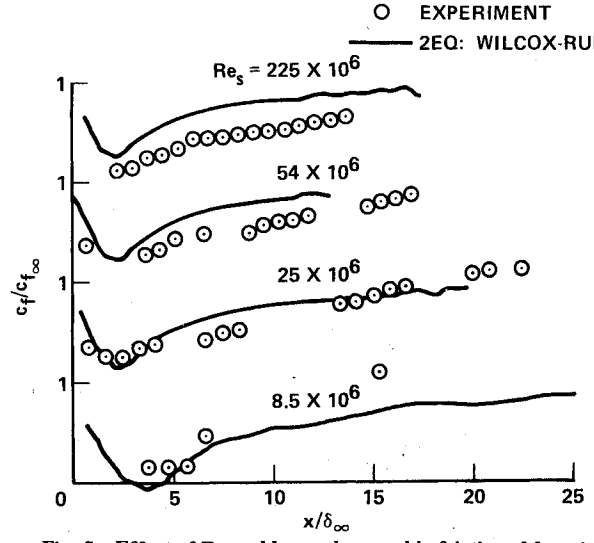

Fig. 5 Effect of Reynolds number on skin friction, $M_\infty = 1.42$.

calculations also illustrate these trends and indicate that the flow is separated for the lowest Reynolds number. Again, separation could not be confirmed with either the c_f or the flow direction data.

Conclusions

The results of the present investigation illustrate the sensitivity of the normal shock-wave/turbulent boundary-layer interaction to variations in Mach and Reynolds number for this flow. The Wilcox-Rubesin turbulence model provides a good representation of these effects for both the wall pressure and skin friction.

References

[1] Seddon, J., "The Flow Produced by Interaction of a Turbulent Boundary Layer with a Normal Shock Wave of Strength Sufficient to Cause Separation," ARC R&M No. 3502, March 1960.

[2] Mateer, G. G., Brosh, A., and Viegas, J. R., "A Normal-Shock-Wave Turbulent Boundary-Layer Interaction at Transonic Speeds," AIAA Paper 76-161, Washington, D.C., Jan. 1976.

[3] Viegas, J. R. and Horstman, C. C., "Comparison of Multi-equation Turbulence Models for Several Shock Separated Boundary-Layer Interaction Flows," AIAA Paper 78-1165, Seattle, Wash., July 1978.

[4] Wilcox, D. C. and Rubesin, M. W., "Progress in Turbulence Modeling for Complex Flowfields," NASA TP-1517, 1980.

[5] McDevitt, J. B., Levy, L. L., Jr., and Deiwert, G. S., "Transonic Flow About a Thick Circular-Arc Airfoil," AIAA Paper 75-878, Hartford, Conn., June 1975.

[6] Mateer, G. G. and Viegas, J. R., "Effect of Mach and Reynolds Numbers on a Normal Shock-Wave/Turbulent Boundary-Layer Interaction," AIAA Paper 79-1502, Williamsburg, Va., July 1979.

Downwash Impingement

B. N. Pamadi*
Indian Institute of Technology, Bombay, India

Introduction

WHEN operating over unprepared terrain, VTOL configurations are known to raise appreciable dust and debris. This not only results in loss of visibility for the pilot but also structural damage to propeller or engine compressor blading when they are hit by the sand particles or gravel lifted from the ground by the downwash impingement (Fig. 1).

Kuhn's studies[1] have shown that the bulk of the erosion or entrainment occurs close to the stagnation point and is confined to a region where the local surface dynamic pressure ($\frac{1}{2}\rho U^2$) exceeds a critical value. For dry sand and loose dirt, he finds that the critical surface dynamic pressure ranges 50-150 N/m^2. The dynamic pressure on the surface rises from zero at the stagnation point to a peak ($\frac{1}{2}\rho U_m^2$) at a point where the static pressure gradient vanishes and then starts falling off due to viscous decay (Fig. 1a). The conditions for incipient erosion are thus determined at the location of peak surface dynamic pressure. Kuhn's observations also reveal that the larger particles are predominantly rolled along the surface while the smaller ones are lifted from the ground.

The sand or dirt particles which are entrained are initially immersed in the boundary layer of the ground. The rolling of the particles occurs when the aerodynamic drag D exceeds the frictional force μW (drag entrainment) and the raising from the ground occurs if the aerodynamic lift L exceeds the particle weight W (lift entrainment). The particles develop lift because they are subjected to shear flow in the boundary layer.

For downwash flow with a uniform velocity distribution, Vidal[2] has developed some criteria for predicting lift and drag entrainment. His results are based upon the classical stagnation point boundary layer solution,[3] applicable to an uniform impinging flow of infinite extent. However, the downwash flow on leaving the jet nozzle has spread and decay characteristics similar to those of a free turbulent jet. In view of this, Vidal's analysis is restricted to low operating heights where the jet mixing effects are small and the velocity is nearly uniform (potential core). The experimental investigations of free jet impingement on normal surface also show that the classical stagnation point solution is applicable only to a small region around the stagnation point.[4,5] Reference 6 reports a more accurate solution for the ground boundary layer in the jet impingement region. Based upon this solution, Vidal's entrainment criteria are extended and presented here in a form applicable for any operating height above the ground surface. These results are in reasonably good agreement with Kuhn's experimental findings.

Criteria for Particle Entrainment

Vidal has given the following criteria,

Drag entrainment:

$$\frac{\rho_s g \delta_0}{\frac{1}{2}\rho U^2} \leq \frac{3}{2\sqrt{2}} C_D \left(\frac{u_0}{U}\right)^2 \left(\frac{\delta_0}{a}\right) \tag{1}$$

where $D/W \geq \mu$, $\mu = 1/\sqrt{2}$, and $C_D = 0.5$.

Lift entrainment:

$$\frac{\rho_s g \delta_0}{\frac{1}{2}\rho U^2} \leq \frac{u_0}{U}\left[\frac{9}{32}\frac{\delta_0}{a}\frac{u_0}{U} + 0.6723\frac{\delta_0}{U}\frac{du_0}{dz}\right] \tag{2}$$

where $L \geq W$ and $W = 4\pi/3\,\rho_s g a^3$.

The quantity $\rho_s g \delta_0 / \frac{1}{2}\rho U^2$ has been termed the loading parameter by Vidal and the same definition will be continued here. This definition of loading parameter is based upon the local dynamic pressure. Hence the loading parameter assumes an infinite value at stagnation point and decreases steadily outward. This parameter can be redefined in terms of maximum surface dynamic pressure ($\frac{1}{2}\rho U_m^2$), which is also equal to dynamic pressure on the free jet axis at an upstream distance, ($z = Z_\infty$) where the effect of the ground surface is negligible. This has the advantage that not only the loading parameter becomes constant with respect to radial distance,

Received May 29, 1979; revision received Nov. 30, 1979.

Index categories: Jets, Wakes, and Viscid-Inviscid Flow Interactions; Aerodynamics; Configuration Designs.

*Assistant Professor, Dept. of Aeronautical Engineering.